J Vet Sci. 2025 Sep;26(5):e64
https://doi.org/10.4142/jvs.25077
pISSN 1229-845X·eISSN 1976-555X

Journal of Veterinary Science

Research Report

Molecular and Cellular Biology

Check for updates

Exosomal miRNA profiling in chickens infected with highly and low pathogenic avian influenza viruses

Chaeeun Kim [1], **Thi Hoai Phan** [1], **Thi Hao Vu** [2], **Anh Duc Truong** [2], **Hyun Soon Lillehoj** [3], **Yeong Ho Hong** [1,*]

[1]Department of Animal Science and Technology, Chung-Ang University, Anseong 17546, Korea
[2]Department of Biochemistry and Immunology, National Institute of Veterinary Research, Hanoi 100000, Vietnam
[3]Animal Biosciences and Biotechnology Laboratory, Agricultural Research Services, United States Department of Agriculture, Beltsville, MD 20705, USA

OPEN ACCESS

Received: Apr 8, 2025
Revised: Jul 14, 2025
Accepted: Jul 23, 2025
Published online: Aug 28, 2025

***Corresponding author:**
Yeong Ho Hong
Department of Animal Science and Technology, Chung-Ang University, 4726 Seodong-daero, Daedeok-myeon, Anseong 17546, Korea.
Email: yhong@cau.ac.kr
https://orcid.org/0000-0002-4510-7851

© 2025 The Korean Society of Veterinary Science
This is an Open Access article distributed under the terms of the Creative Commons Attribution Non-Commercial License (https://creativecommons.org/licenses/by-nc/4.0) which permits unrestricted non-commercial use, distribution, and reproduction in any medium, provided the original work is properly cited.

ABSTRACT

Importance: Avian influenza virus (AIV) has emerged as a serious threat worldwide. In poultry, AIV can be divided into highly pathogenic AIV (HPAIV) and low pathogenic AIV (LPAIV). Exosomes are small vesicles released from donor cells that transmit cargo such as microRNAs (miRNAs), where exosomal miRNA can regulate target gene expression.
Objective: By profiling exosomal miRNAs from chickens infected with HPAIV and LPAIV, we provide insights into the immunological functions of exosomal miRNAs in AIV infection as well as into the development of strategies for its control.
Methods: This study analyzed the exosomal miRNA expression profiles of non-infected, LPAIV-infected, and HPAIV-infected chickens using small RNA sequencing. miRDB and Gene Ontology (GO) were used to predict immune-related target genes, and GO and Kyoto Encyclopedia of Genes and Genomes (KEGG) analyses were performed. Reverse transcription quantitative polymerase chain reaction was conducted to validate the expression levels of miRNAs (gga-miR-1434, gga-miR-1662, gga-miR-1559-5p, and gga-miR-375).
Results: We identified 148 DE miRNAs in total: 103 in LPAIV-EXO vs. CTRL-EXO, 54 in HPAIV-EXO vs. CTRL-EXO, and 98 in HPAIV-EXO vs. LPAIV-EXO, with partial overlap among groups. In the GO and KEGG analyses, the mitogen-activated protein kinase signaling pathway was the most enriched pathway in all comparisons.
Conclusions and Relevance: This report provides insight into the molecular mechanisms by which exosomal miRNAs are related to immune-related pathways in HPAIV and LPAIV infections and is expected to be helpful for novel vaccine development and useful biomarkers for virus infections.

Keywords: Exosome; immune related miRNA; avian influenza virus; RNA-Seq; chicken

Generated by XmlInkpress

ORCID iDs

Chaeeun Kim
https://orcid.org/0009-0002-9482-5398
Thi Hoai Phan
https://orcid.org/0009-0001-2970-1981
Thi Hao Vu
https://orcid.org/0000-0001-9098-6990
Anh Duc Truong
https://orcid.org/0000-0002-2472-8165
Hyun Soon Lillehoj
https://orcid.org/0000-0001-7755-6216
Yeong Ho Hong
https://orcid.org/0000-0002-4510-7851

Author Contributions

Conceptualization: Hong YH, Kim C; Data curation: Kim C, Vu TH, Phan TH; Formal analysis: Kim C, Truong AD; Funding acquisition: Hong YH; Investigation: Kim C, Truong AD; Methodology: Kim C, Phan TH, Vu TH; Project administration: Hong YH; Resources: Truong AD; Software: Kim C; Supervision: Hong YH; Validation: Kim C, Vu TH; Visualization: Kim C; Writing - original draft: Kim C; Writing - review & editing: Kim C, Hong YH, Lillehoj HS.

Conflict of Interest

The authors declare no conflicts of interest.

Data Availability Statement

The datasets used and/or analysed during the current study are available from the corresponding author upon reasonable request.

Funding

This research was funded by the National Research Foundation grant (NRF-2021R1A2C2005236) of the Republic of Korea.

INTRODUCTION

Avian influenza virus (AIV) can cause a disease of great importance for animal and human health, especially in the poultry industry, as it reduces productivity [1]. AIV belongs to the *Orthomyxoviridase* family and is a single-stranded negative RNA virus; infections begins in the nasal and tracheal airways and spread to the upper and lower respiratory tracts [2]. These viruses have animal reservoirs, such as mice, swine, and birds, and avian-origin influenza virus occasionally transfer to other species and spread to humans, raising concerns from a global public health perspective that they may cause zoonotic diseases. AIVs can be classified as highly pathogenic avian influenza virus (HPAIV) and low pathogenic avian influenza virus (LPAIV) based on their pathogenesis in poultry [3]. LPAIV is associated with lower mortality rates than HPAIV and thus is considered to have relatively low disease severity, but LPAIV strains (especially the H5 or H7 subtype) may evolve into HPAIV by transmitting to birds. Thus, early detection and suppression strategies will help prevent the spread of the virus in the global poultry industry, as surveillance for LPAIV is essential to prohibit the emergence of new subtypes of HPAIV [4].

Exosomes are small membrane microvesicles with a diameter of 30–120 nm that are derived from several types of cells [5,6]. Exosomes are formed by multivesicular bodies derived from inward budding of late endosomal membranes, and as they are released into the extracellular space, they fuse with the plasma membrane of surrounding cells [7,8]. The most of important function of exosomes is cell-to-cell communication by transferring their contents such as proteins, lipids, DNAs, and microRNAs (miRNAs) to recipient cells. In viral infections, the pathological cells can carry their viral particles, non-coding RNAs (ncRNAs), and spread pathogenic agents as well as ncRNAs to the host's body. However, by utilizing these characteristics, exosomes derived from healthy donor tissue without infectious agents can be used as a therapeutic method and can prevent infection [9].

miRNAs within exosomes or exosomal miRNAs also pass into the recipient cells and form a RISC complex by targeting the miRNA 3'UTR (Untranslated region) and AGO2 protein to degrade target genes or prevent translation [10]. Exosomal miRNAs induce host defense systems by delivering cargo and have antiviral activity [7,11].

In several studies, it has been confirmed that miRNAs derived from exosomes can be effective strategies for regulating influenza virus [9,12]. Severe acute respiratory syndrome coronavirus 2, which caused a pandemic of acute respiratory diseases, has recently become a global threat. Exosomal miRNAs from mesenchymal stem cells, miR-125a-3p and miR-125b-3p, facilitate reducing the expression of inflammatory cytokines and chemokines by targeting multiple regions in the 3'UTR of specific mRNAs and also regulate the coagulation cascade and cell death [9].

In particular, in our previous study, we isolated exosomes from Ri chickens, which are local household chickens in Vietnam, and divided them into groups that were resistant or susceptible to AIV by genotyping the Mx and BF2 genes; we found that differentially expressed (DE) miRNAs derived from exosomes were involved in the mitogen-activated protein kinase (MAPK) signaling pathway, a central pathway of the immune system. In addition, we analyzed exosomal miRNAs in exosomes from White Leghorn chickens infected with HPAIV H5N1 and found that 10 DE miRNAs were significantly expressed between uninfected and HPAIV H5N1-infected chickens. However, there are still far more

studies focused on HPAIV than LPAIV. LPAIV can lead to more severe loss to global health because of coinfection with other pathogens [13]. Even, LPAI progenitor viruses can directly evolve to HPAIV, and not much research has been done on this to date [14]. Therefore, it is important to understand the mechanism between AIVs and chickens for the development of the avian industry and global health. We accordingly focused on the differences between LPAIV and HPAIV based on pathogenicity through high-throughput miRNA sequencing in exosomes that can perform immunologically important functions as well as on discovering the regulatory mechanisms of exosomal miRNAs.

METHODS

Animal experiments

Twenty-one four-week-old specific-pathogen-free Brown Leghorn chickens, which were obtained from the National Institute of Animal Science in Hanoi, Vietnam, were infected with AIV. The animal infection experiment was performed in the biosafety level 2 plus facility of our collaborative laboratory in the Department of Biochemistry and Immunology, National Institute of Veterinary Research, Vietnam. For LPAIV infection, 7 chickens were treated intranasal inoculation of 200 uL of harvested allantoic fluid from infected eggs, including 1×10^4 50% egg infectious dose [15] of A/Chicken/Vietnam/NA11/2021 (H5N6). For HPAIV infection, seven chickens were infected with A/chicken/Vietnam/NA01/2019 (H5N1) under the same conditions as LPAIV. Both animal infection experiments were approved the guidelines of the World Health Organization for Animal Health. The other seven non-infected chickens were set as the control group. After three days of AIV treatment, blood samples from the wing veins of the chickens were collected for exosome isolation. This study was conducted in compliance with the institutional rules for the care and ethical use of laboratory animals, using a protocol approved by the Ministry of Agriculture and Rural Development, Vietnam (TCVN 8402:2010/TCVN 8400-26:2014).

Exosome isolation and characterization

Exosomes were isolated from the serum of non-infected chickens (CTRL-EXO), LPAIV-infected chickens (LPAIV-EXO), HPAIV-infected chickens (HPAIV-EXO) using Total Exosome Isolation Reagent (Invitrogen, USA), according to previously described methods [16]. The size of the exosomes was measured with a nanoparticle analyzer (SZ-100; HORIBA, Japan). Detection of the exosomal markers CD9 (#13174; Cell Signaling Technology, USA) and CD81 (#56039; Cell Signaling Technology) was conducted by western blotting.

Exosomal RNA extraction and small RNA sequencing

RNA within the exosomes from three groups (CTRL-EXO, LPAIV-EXO, and HPAIV-EXO) was extracted using miRNeasy Serum/Plasma Kit (Qiagen, Germany) according to the manufacturer's protocol. Library construction was conducted using SMARTer smRNA-Seq for Illumina Kit per the manufacturer's protocol. Then, small RNA sequencing was performed using Hiseq 2500 System (Illumina Inc., USA) at Macrogen (Korea).

Bioinformatics analysis

After sequencing, the raw sequence reads were filtered with FastQC v0.11.9 based on quality (http://www.bioinformatics.babraham.ac.uk/projects/fastqc/). The adapter sequences are trimmed from raw data. The trimmed reads and non-adapter reads were used to analyze the long target (≥ 50 bp), and these processed reads produced unique cluster by assembling. Unique

clustered reads were aligned to the reference genome miRbase v22.1 (http://www.mirbase.org/), and the ncRNA database RNAcentral 14.0 (https://rnacentral.org/) was used to sort known miRNA and other types of RNA including tRNA, snRNA, and snoRNA, etc. Final processed reads were aligned to the GRCg6a reference genome by Bowtie and STAR 2.6.0c using RSEM version v1.3.1 (https://deweylab.github.io/RSEM/). Both known and novel miRNA were predicted by miRDeep2 (https://www.mdc-berlin.de/content/mirdeep2-documentation), and other miRNAs matching RNA central were aligned using Bowtie 1.1.2 (http://bowtie-bio.sourceforge.net/index.shtml) (target smRNA, < 50 nt) and HISAT2 version 2.1.0, Bowtie2 2.3.4.1 (https://ccb.jhu.edu/software/hisat2/index.shtml) (target smRNA, ≥ 50 nt).

DE miRNA, Gene Ontology (GO) and Kyoto Encyclopedia of Genes and Genomes (KEGG) enrichment analysis

The read counts for each miRNA describe the abundance of each miRNA extracted from mapped miRNAs. To sort DE miRNA among samples, the read count values of mature miRNAs acquired from miRDeep2 were used as raw data. Data pre-processing was performed to filter out low-quality miRNAs, and read count data were normalized in the edgeR library using the Trimmed Mean of M-value method. Statistical analysis of DE miRNAs was conducted using Fold Change and exactTest using edgeR (Empirical Analysis of Digital Gene Expression Data in R) and hierarchical clustering. Significant results were collected on conditions of a |fold change| ≥2 and an exactTest raw p value < 0.05. Hierarchical clustering analysis to select significant miRNAs was performed to group similar samples and mature miRNAs. The target genes of DE miRNAs were predicted using miRDB (https://mirdb.org/). Target genes with a target score over 80 were selected, and GO analysis (https://geneontology.org/) was used to predict immune-related genes among them. The GO enrichment analysis and KEGG pathway enrichment analysis were conducted with gProfiler (http://biit.cs.ut.ee/gprofiler/gost). Among them, the top 10 significantly enriched terms were chosen.

Reverse transcription quantitative PCR (RT-qPCR) validation of miRNA

The forward primers for validation of each miRNA were supplied by TB Green Advantage qPCR Premix (Takara Bio Inc., Japan). Known chicken miRNA sequences were acquired from miRbase (https://www.mirbase.org/). The oligonucleotide primers for RT-qPCR analysis were designed based on full-length mature miRNA sequences and synthesized with Genotech (Korea), as indicated in **Supplementary Table 1**. cDNA synthesis was conducted using Mir-X miRNA First-Strand Synthesis and TB Green qRT-PCR (Takara Bio Inc.) according to the manufacturer's protocol, and synthesized cDNA was consumed as a template for RT-qPCR. The expression of miRNA was confirmed using TB Green Advantage qPCR Premix (Takara Bio Inc.) in the CFX Connect Real-Time PCR Detection System (Bio-Rad, USA) according to the manufacturer's protocol. To analyze miRNA expression, 12.5 uL of TB Green, 0.5 uL of forward primer, 0.5 uL of universal primer, 0.5 uL of Rox dye, 1 uL of 100 ng template DNA, and nuclease-free water up to 25 uL were used. The cycling program was as follows: The mixture was incubated at 95°C for 10 min, followed by 40 cycles of 95°C for 5 sec, 60°C for 20 sec, and 65°C for 5 sec. The expression data from RT-qPCR were evaluated using the $2^{-\Delta\Delta Ct}$ method [17] and normalized with U1A. All RT-qPCR analyses were conducted as individual experiments performed in triplicate.

RESULTS

Isolation and characterization of exosomes

Exosomes isolated from the blood serum of non-infected, LPAIV-infected, and HPAIV-infected chickens were characterized based on particle size and surface markers (**Fig. 1**). The size distribution of CTRL-EXO, LPAIV-EXO, and HPAIV-EXO ranged from 82.33 to 171.25 nm (**Fig. 1A**). The exosomal protein marker CD9 was detected in each exosome (CTRL-EXO, LPAIV-EXO, and HPAIV-EXO) by western blotting (**Fig. 1B**). CD81 was analyzed under the same experimental conditions; however, reliable results could not be obtained (not shown).

Analysis of exosomal miRNA

Small RNA sequencing was conducted on control samples as well as LPAIV- and HPAIV-infected samples. The total number of reads in CTRL-EXO was 7,963,617, and the read bases was 3.5 Gbp. In LPAIV-EXO, 72,311,636 reads were produced, and the total number of read bases was 3.7 Gbp. Finally, in HPAIV-EXO, 71,749,915 reads were produced and 3.7 Gbp of bases were sequenced. The clean read pairs with a Phred score of Q30 in each sample comparison were 88.99%, 87.97%, and 89.86% for CTRL-EXO, LPAIV-EXO, and HPAIV-EXO, respectively. The read length distribution of mature miRNAs in each sample was 20–25 nt (**Supplementary Fig. 1**). After trimming and quality control, processed reads were sequentially aligned to the reference genome miRBase v22.1 and ncRNA database (RNAcentral release 14.0) to classify known miRNAs and other types of RNA such as piRNA, tRNA, snRNA, and snoRNA, etc. (**Supplementary Fig. 2**).

In CTRL-EXO, among 45,764,691 processed reads, a total of 83.11% (38,036,146) of the reads were mapped to the reference genome, which defined 328 known miRNAs. In addition, in LPAIV-EXO, 86.36% (46,121,451) of the reads were mapped, and 365 known miRNAs were found. Finally, in HPAIV-EXO, 80.1% (36,142,185) reads were mapped, and 339 known miRNAs were detected (**Table 1**).

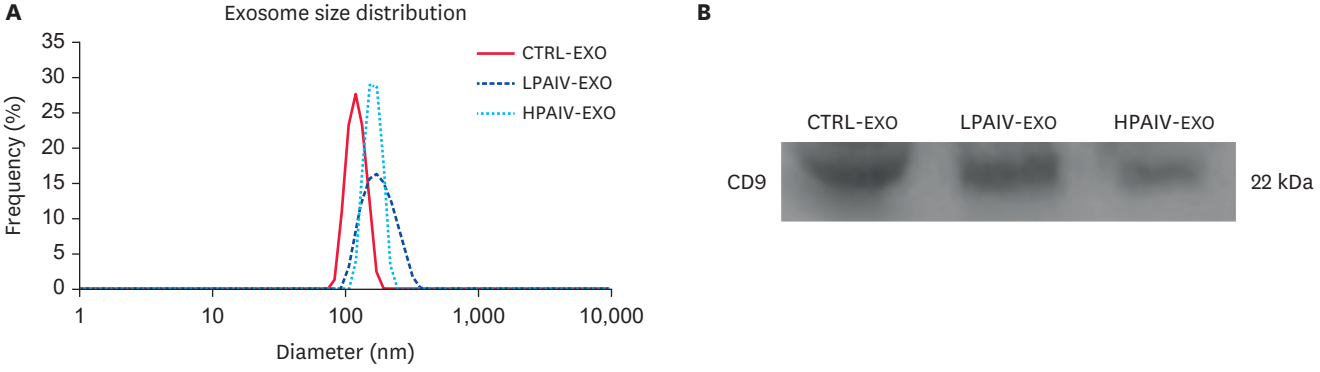


Fig. 1. Characterization of exosomes. (A) Particle size distribution of the exosomes. (B) Exosomal marker CD9 detection by western blotting analysis. CTRL-EXO, exosomes extracted from non-infected chickens; LPAIV-EXO, exosomes extracted from low pathogenic avian influenza virus-infected chickens; HPAIV-EXO, exosomes extracted from highly pathogenic avian influenza virus-infected chickens.

Table 1. Quality assessment of raw small RNA sequencing data from CTRL-EXO, LPAIV-EXO, and HPAIV-EXO

Sample	Total read bases	Total reads	Processed reads	Mapped reads	Q30 (%)	Known miRNA
CTRL-EXO	3,466,144,467	67,963,617	45,764,691	38,036,146 (83.11%)	88.99	328
LPAIV-EXO	3,687,893,436	72,311,636	53,407,617	46,121,451 (86.36%)	89.86	365
HPAIV-EXO	3,659,245,665	71,749,915	45,119,724	36,142,185 (80.1%)	87.97	339

CTRL-EXO, exosomes extracted from non-infected chickens; LPAIV-EXO, exosomes extracted from low pathogenic avian influenza virus-infected chickens; HPAIV-EXO, exosomes extracted from highly pathogenic avian influenza virus-infected chickens; miRNA, microRNA.

The DE miRNAs yielded a total of 148 miRNAs among the three comparison groups (LPAIV-EXO vs. CTRL-EXO, HPAIV-EXO vs. CTRL-EXO, and HPAIV-EXO vs. LPAIV-EXO) based on the $\log_2$ fold change and at significance level of $p < 0.05$ (**Supplementary Table 2**). Based on these result data, the volcano plot in **Fig. 2** shows differences in the expression levels of DE miRNAs in each of the three comparison groups. Based on a |fold change| ≥ 2 and a raw *p* value < 0.05, red dots represent upregulated DE miRNAs, while blue dots indicate downregulated DE miRNAs. In the LPAIV-EXO vs. CTRL-EXO comparison, a total of 103 DE miRNAs including 57 upregulated DE miRNAs and 46 downregulated DE miRNAs were identified (**Fig. 2A**, **Supplementary Table 2**). A total of 54 DE miRNAs including 57 upregulated and 46 downregulated miRNAs were identified in the HPAIV-EXO vs. CTRL-EXO comparison (**Fig. 2B**, **Supplementary Table 2**). A total of the 98 DE miRNAs including 45 upregulated and 53 downregulated miRNAs were identified in the HPAIV-EXO vs. LPAIV-EXO comparison (**Fig. 2C**, **Supplementary Table 2**). Furthermore, a total of 148 miRNAs were analyzed among the 3 samples by hierarchical clustering (**Fig. 3A**). A mature miRNA expression pattern in the 3 samples (CTRL-EXO, LPAIV-EXO, and HPAIV-EXO) was visualized with sample-specific differences. In particular, the LPAIV-EXO vs. CTRL-EXO comparison showed the opposite expression pattern of miRNAs.

The three groups were compared, and co-expressed miRNAs and specific DE miRNAs are represented using a Venn diagram in **Fig. 3B**. Twelve DE miRNAs (gga-miR-1434, gga-miR-1559-5p, gga-miR-1662, gga-miR-1682, gga-miR-184-3p, gga-miR-200a-5p, gga-miR-200b-5p, gga-miR-214, gga-miR-34b-3p, gga-miR-34c-3p, gga-miR-375, and gga-miR-7b) were commonly expressed in all three groups. In the LPAIV-EXO vs. CTRL-EXO and HPAIV-EXO vs. CTRL-EXO comparisons, 18 DE miRNAs were significantly expressed. Fifty-four DE miRNAs were discovered in the LPAIV-EXO vs. CTRL-EXO and HPAIV-EXO vs. LPAIV-EXO comparisons. The overlapping DE miRNAs between two groups (HPAIV-EXO vs. CTRL-EXO and HPAIV-EXO vs. LPAIV-EXO) included 11 DE miRNAs. These results suggest that exosomal miRNA profiles undergo dynamic changes during LPAIV infection that during HPAIV infection when compared to the control.

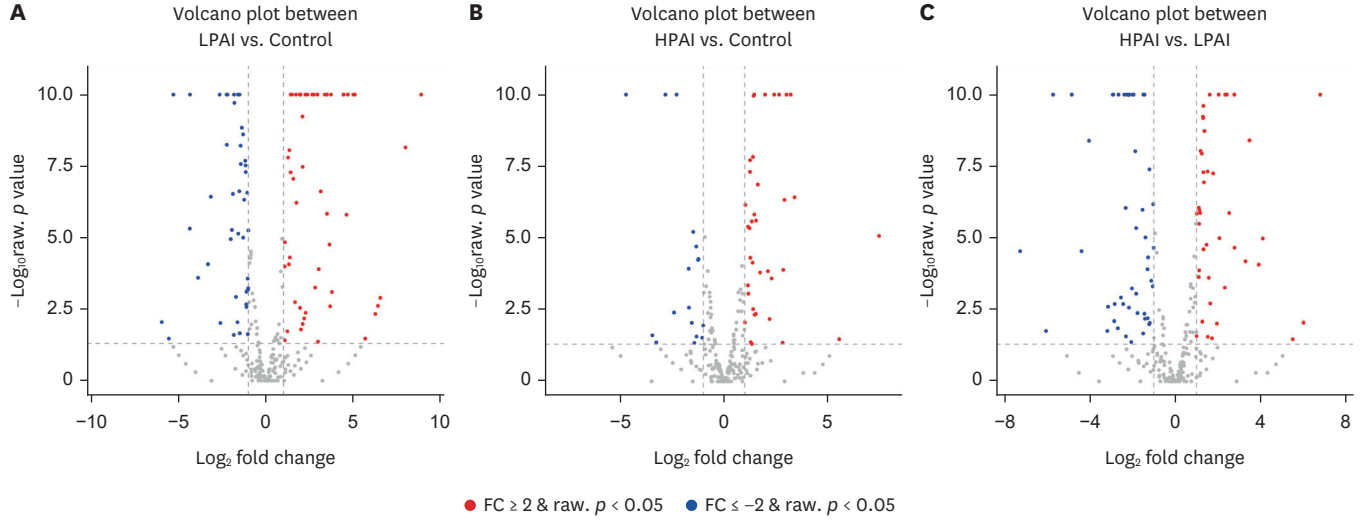


Fig. 2. Volcano plot of exosomal DE miRNAs among CTRL-EXO, LPAIV-EXO, and HPAIV-EXO in the three comparison groups, (A) LPAIV-EXO vs. CTRL-EXO, (B) HPAIV-EXO vs. CTRL-EXO, and (C) HPAIV-EXO vs. LPAIV-EXO.
DE, differentially expressed; miRNA, microRNA; CTRL-EXO, exosomes extracted from non-infected chickens; LPAIV-EXO, exosomes extracted from low pathogenic avian influenza virus-infected chickens; HPAIV-EXO, exosomes extracted from highly pathogenic avian influenza virus-infected chickens; FC, fold change.

https://doi.org/10.4142/jvs.25077

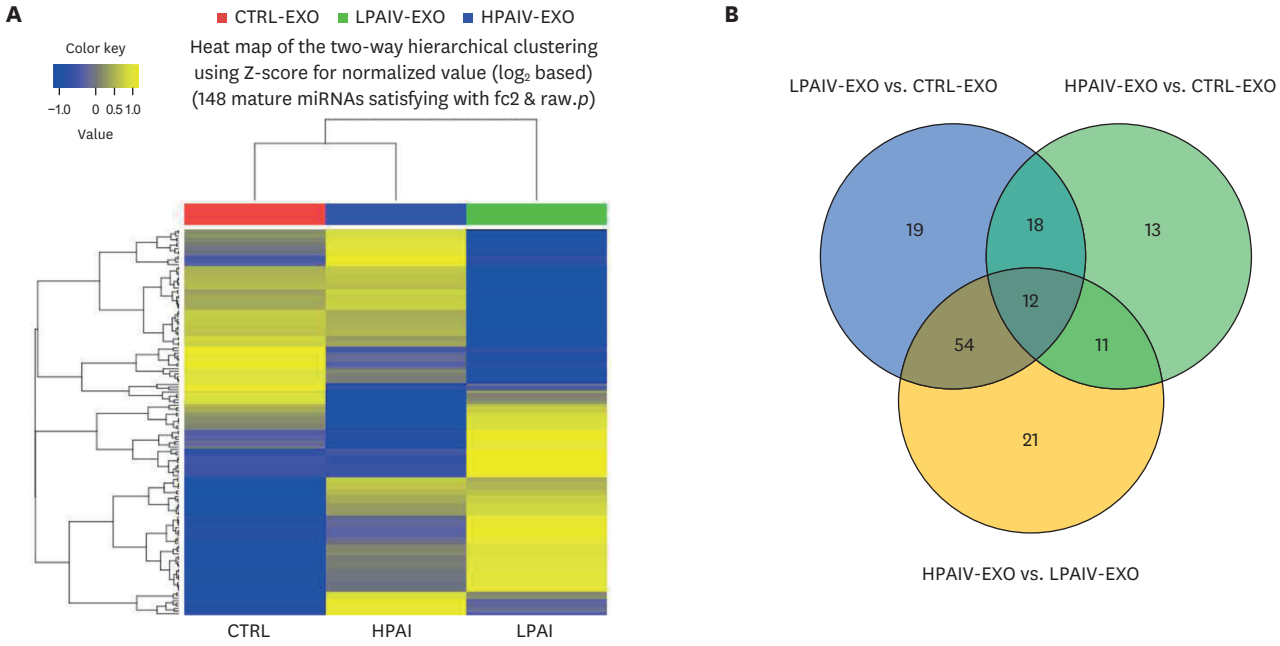


Fig. 3. Heat map and Venn diagram for differentially expressed miRNAs. (A) Heat map with hierarchical clustering results of the three comparison groups using the Z-score for the normalizing value (log2-based) with 148 mature miRNAs. (B) Venn diagram of exosomal DE miRNAs in different comparisons (LPAIV-EXO vs. CTRL-EXO, HPAIV-EXO vs. CTRL-EXO, and HPAIV-EXO vs. LPAIV-EXO).
miRNA, microRNA; DE, differentially expressed; LPAIV-EXO, exosomes extracted from low pathogenic avian influenza virus-infected chickens; CTRL-EXO, exosomes extracted from non-infected chickens; HPAIV-EXO, exosomes extracted from highly pathogenic avian influenza virus-infected chickens.

Immune-related target gene prediction and GO and KEGG pathway enrichment analyses

Among the target genes found using miRDB in the comparison of the three groups, immune-related target genes were selected through GO (**Supplementary Table 3**). There were no immune-related target genes on gga-miR-1559-5p, gga-miR-1434, or gga-miR-184-3p in common.

GO and KEGG pathway enrichment analyses of DE miRNAs were performed to represent immune-related functional terms by comparing the 3 groups, and the top 10 significantly enriched terms that were chosen in the GO and KEGG pathway analyses included molecular function, biological processes, and cellular components. GO analysis was conducted on 6,620 target genes in the LPAIV-EXO vs. CTRL-EXO group, which were enriched into 72 GO terms in molecular functions, 480 GO terms in biological processes, and 80 GO terms in cellular components (**Supplementary Table 4**). **Supplementary Fig. 3A** shows 10 KEGG pathways including the MAPK signaling pathway, Wnt signaling pathway, Hedgehog signaling pathway, and ErbB signaling pathway, which are all pathways related to viral infection and inflammation.

In the HPAIV-EXO vs. CTRL-EXO group, 5,674 target genes were subcategorized into 76, 403, and 61 GO terms from molecular functions, biological processes, and cellular components, respectively (**Supplementary Table 4**). Seven KEGG pathways were identified, and the most enriched pathway was the MAPK signaling pathway (**Supplementary Fig. 3B**). A total of 6,438 target genes were identified in the HPAIV-EXO group compared with the LPAIV-EXO group, which included 60 GO terms in molecular function, 439 GO terms in biological processes, and 64 GO terms in cellular components (**Supplementary Table 4**). KEGG enrichment analysis revealed six enriched pathways including the MAPK signaling pathway, Wnt signaling pathway, and Hedgehog signaling pathway, as shown in **Fig. 4**.

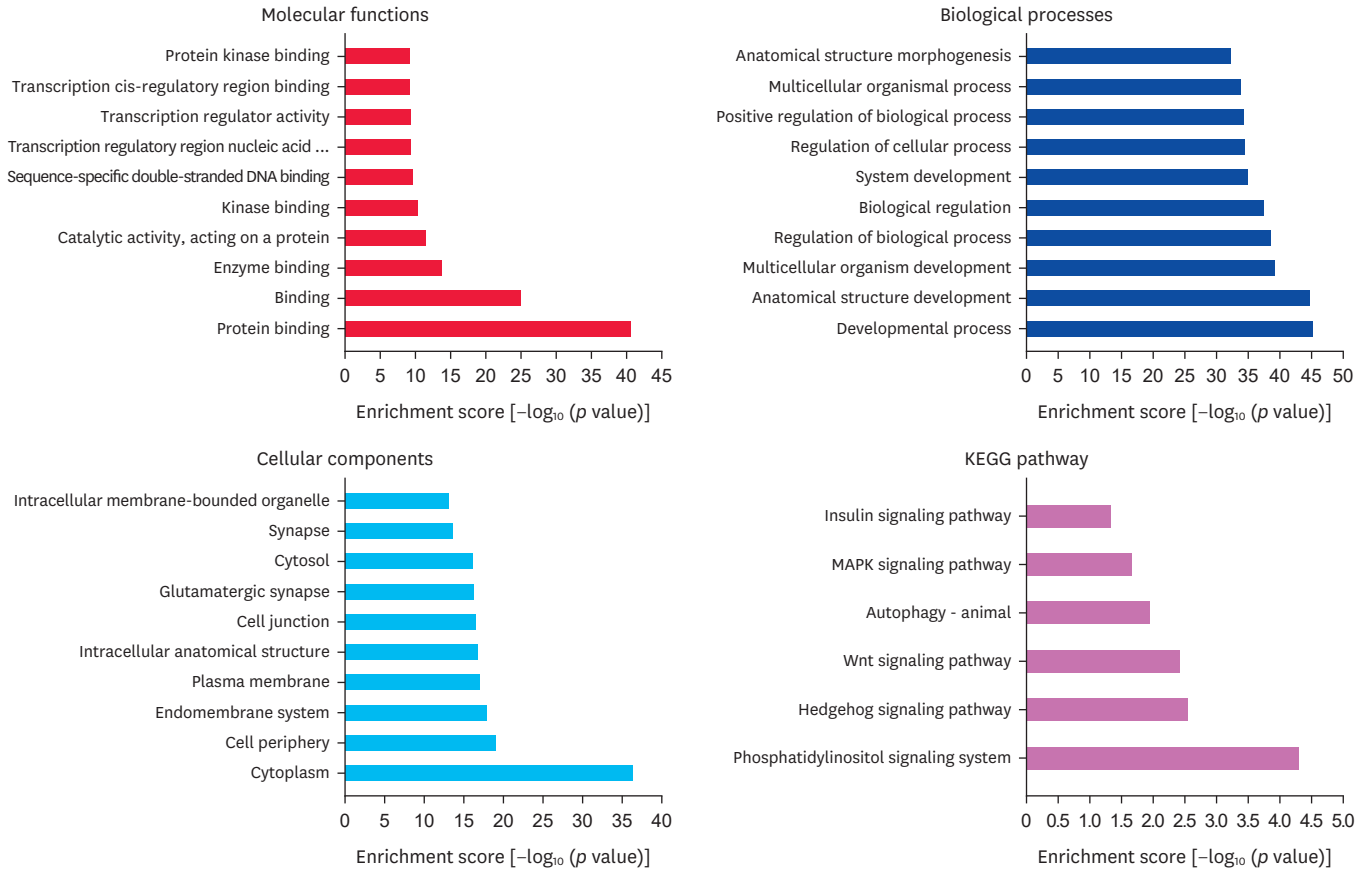


Fig. 4. Top 10 enriched GO and KEGG pathways for DE miRNAs. HPAIV-EXO vs. LPAIV-EXO comparison with molecular functions, biological processes, cellular components, and the KEGG pathway.
GO, Gene Ontology; KEGG, Kyoto Encyclopedia of Genes and Genomes; DE, differentially expressed; miRNA, microRNA; HPAIV-EXO, exosomes extracted from highly pathogenic avian influenza virus-infected chickens; LPAIV-EXO, exosomes extracted from low pathogenic avian influenza virus-infected chickens; CTRL-EXO, exosomes extracted from non-infected chickens.

KEGG pathway enrichment analysis showed that the target genes of the DE miRNAs were commonly involved in the immune-related pathway, the MAPK signaling pathway, the Hedgehog signaling pathway, and autophagy in the three comparison groups.

Validation of DE miRNAs by RT-qPCR

To confirm the small-scale RNA sequencing results, miRNAs commonly expressed in all three groups were selected and validated through RT-qPCR analysis. The expression level of gga-miR-1434 was downregulated with a 0.21 fold change in LPAIV-EXO and a 0.54 fold change in HPAIV-EXO compared with CTRL-EXO. In gga-miR-1662, the expression patterns were upregulated with a 4.79 fold change in LPAIV-EXO and 1.99 fold change in HPAIV-EXO compared with CTRL-EXO. In addition, gga-miR-1559-5p showed an expression pattern similar to gga-miR-1434. The expression pattern of gga-miR-375 showed a similar pattern to that of gga-miR-1662; LPAIV-EXO had the highest expression compared with CTRL-EXO and HPAIV-EXO. Furthermore, gga-miR-1434 and gga-miR-1559-5p also showed similar expression patterns and tended to decrease in infected exosomes (LPAIV-EXO, HPAIV-EXO) compared with CTRL-EXO. Finally, all miRNA expression patterns except for those of gga-miR-1559-5p followed the sequencing results.

https://doi.org/10.4142/jvs.25077

DISCUSSION

Exosomes have emerged as crucial mediators of cellular communication, attracting significant attention for their potential in developing novel therapeutic approaches by elucidating their underlying mechanisms. In a previous study, we analyzed exosomal miRNA profiles derived from HPAIV-infected White Leghorn chickens through small RNA sequencing [18]. In this study, we aimed to compare the profiling of exosomal miRNAs that vary with pathogenicity among noninfected (CTRL-EXO), LPAIV-infected (LPAIV-EXO), and HPAIV-infected (HPAIV-EXO) groups and to investigate the functions of immune-related miRNAs.

In this study, we report the profiling of exosomal miRNA from non-infected, LPAIV-infected or HPAIV-infected chickens. A total of 148 DE miRNAs derived from exosomes were identified through small RNA sequencing. Of these, 98 DE miRNAs were classified in the HPAIV-EXO vs. LPAIV-EXO comparison, 54 DE miRNAs were included in the HPAIV-EXO vs. CTRL-EXO comparison, and 103 DE miRNAs were involved in the in LPAIV-EXO vs. CTRL-EXO comparison.

In a previous study, Wu et al. [19] revealed that during Fawl adenovirus aerotype 4 infection, gga-miR-1662 played important roles in viral and bacterial infections and influenced immune responses in *Salmonella enterica* infections by targeting interleukin-24. Furthermore, gga-miR-7b has been found to affect virus attachment and release by generating new infectious viral particles in AIV-infected chicken lungs [20]. Moreover, it has been reported that gga-miR-7b is associated with the pathogenesis of infectious bronchitis virus depending on the virulence of the virus strain [21]. In addition, our previous study [22] revealed that gga-miR-214 in exosomes of two groups of Ri chickens that were either resistant or susceptible to HPAIV infection was involved in viral infection by showing upregulated pattern in HPAIV-infected samples compared with control samples. Moreover, our results also showed that gga-miR-214 had higher expression in infected samples (LPAIV-EXO, HPAIV-EXO) than in CTRL-EXO (**Supplementary Table 2**). However, since LPAIV-EXO showed a higher fold change than HPAIV-EXO, we can expect that gga-miR-214 would be more significant and sensitive in LPAIV infection. Furthermore, gga-miR-375 has been identified a novel tumor suppressor in avian leukosis virus infection, and has been confirmed to induce changes in tumor cell status via regulation of its expression. Based on this, it was revealed that it plays an important role in tumorigenesis in avian leukosis [23].

These GO and KEGG enrichment analyses revealed that the MAPK signaling pathway was significantly enriched across all comparison groups. These findings suggest that intercellular signaling via exosomes is regulated by the MAPK signaling pathway during AIV infection and that DE miRNAs in exosomes act as mediators of this signaling. The MAPK signaling pathway is a key mediator of cellular programs including cell proliferation, differentiation, development, inflammatory responses, and apoptosis [24] and is also considered a very important factor in maintaining the immune system through its participation in intracellular signaling pathways. Moreover, in mammalian species, it is implicated in all aspects of the immune response including innate immunity, adaptive immunity, cytokine production and differentiation, maturation of various types of immune cells, and cell death when immune function is completed [25,26]. Many reports have already announced that some types of viruses, including influenza A viruses, can activate the p38-MAPK signaling pathway, which is particularly involved in viral replication [27]. HPAIVs, such as H5N1, can prompt

host cell signaling pathways such as the MAPK pathway to induce uncontrolled release of inflammatory cytokines and chemokines, such as in a cytokine storm, which lead to acute lung injuries and acute respiratory distress syndrome. In this process, the MAPK signaling pathway serves as an essential virus sensor signaling cascade [28,29]. In addition, our previous study revealed that exosomal miRNAs from White Leghorns infected with HPAIVs were associated with the MAPK signaling pathway [18]. Based on these findings, exosomal miRNAs were involved in AIVs through the MAPK signaling pathway, which is an important implication for understanding the infectious mechanisms underlying HPAIVs and LPAIVs.

Furthermore, the Hedgehog signaling pathway and autophagy also were commonly associated with the three group comparisons. The Hedgehog signaling pathway is an important signaling pathway involved in tissue homeostasis and developmental processes including embryonic development [30]. However, it has been suggested that it plays a role in modulating the immune response [31], including in viral infections, as it is involved in the function and differentiation of immune cells [32]. Autophagy is recognized as a host defense mechanism against viral infection by modulating immune responses, such as by promoting the degradation of viral components and facilitating the capture and removal of incoming pathogens. In addition, influenza viruses have evolved to activate cellular autophagy processes to evade these host restrictions and promote viral replication and budding [10,33,34]. Overall, GO and KEGG enrichment analyses confirmed that both HPAIV and LPAIV infections involve the MAPK signaling pathway, but some pathways are different. In the HPAIV-EXO vs. CTRL-EXO comparison, the MAPK signaling pathway was the most enriched among the seven identified pathways, supporting its central role in the immune response associated with highly pathogenic viral infections (**Supplementary Fig. 3A**). In contrast, in the LPAIV-EXO vs. CTRL-EXO comparison, pathways such as Wnt and ErbB, in addition to MAPK, were significantly enriched, suggesting a broader modulation of cellular signaling pathways that may be associated with a less severe immunopathological response (**Supplementary Fig. 3B**).

RT-qPCR (**Fig. 5**) suggested that specific miRNAs are selectively regulated in LPAIV and HPAIV infections and that the expression of immune-related genes is modulated by decreases or increases in these miRNAs. However, additional experimental verification is needed to confirm that exosomal miRNAs are involved in immune-related mechanisms by regulating the expression of immune-related genes.

The findings of this study provide important implications for understanding the molecular mechanisms of HPAIV and LPAIV infections as well as the use of noninvasive biomarkers in determining various infection statuses. Furthermore, based on the characteristics of exosomal miRNAs that regulate the expression of specific genes, most genes were associated with the MAPK signaling pathway when comparing the three groups. Although this study highlights the involvement of exosomal miRNAs in the regulation of MAPK signaling pathway during LPAIV and HPAIV infections, it has limitations that require functional validation of the interactions between exosomal miRNAs and signaling pathways. Further experimental studies are needed to confirm these interactions and to clarify the underlying molecular mechanisms.

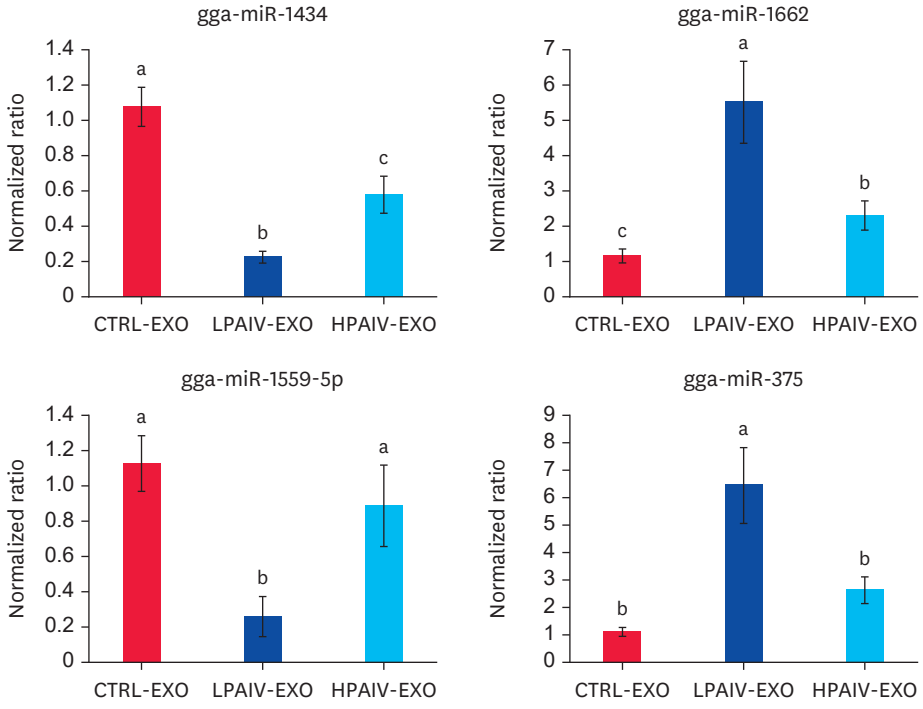


Fig. 5. RT-qPCR validation of exosomal miRNAs. All data are normalized to U1A and are presented as the mean ± standard error of the mean using the $2^{-\Delta\Delta Ct}$ method in triplicate experiments.
RT-qPCR, reverse transcription quantitative polymerase chain reaction; miRNA, microRNA; CTRL-EXO, exosomes extracted from non-infected chickens; LPAIV-EXO, exosomes extracted from low pathogenic avian influenza virus-infected chickens; HPAIV-EXO, exosomes extracted from highly pathogenic avian influenza virus-infected chickens.
[a,b,c]Different lowercase letters above the bars indicate statistical significance ($p < 0.05$) as determined by analysis of variance with Tukey's multiple comparison test.

ACKNOWLEDGMENTS

The authors thank the Department of Biochemistry and Immunology Laboratory of the National Institute of Veterinary Research, Vietnam, for conducting the animal experiments described in this study.

SUPPLEMENTARY MATERIALS

Supplementary Table 1

Primer sequences for reverse transcription quantitative polymerase chain reaction

Supplementary Table 2

Differentially expressed miRNAs list: total 148 miRNAs were identified in 3 groups (CTRL-EXO, LPAIV-EXO, and HPAIV-EXO)

Supplementary Table 3

Immune-related target of exosomal miRNAs in LPAIV-EXO vs. CTRL-EXO, HPAIV-EXO vs. CTRL-EXO, and HPAIV-EXO vs. LPAIV-EXO

Supplementary Table 4

GO and KEGG enrichment analysis of differentially expressed miRNAs between LPAIV-EXO and CTRL-EXO, HPAIV-EXO vs. CTRL-EXO, and HPAIV-EXO vs. LPAIV-EXO

Supplementary Fig. 1

Read length distribution of CTRL-EXO, LPAIV-EXO, and HPAIV-EXO.

Supplementary Fig. 2

RNA composition in (A) CTRL-EXO, (B) LPAIV-EXO, and (C) HPAIV-EXO.

Supplementary Fig. 3

Top 10 enriched GO and KEGG pathways for DE miRNAs. (A) GO and KEGG pathway enrichment analyses of LPAIV-EXO vs. CTRL-EXO and (B) HPAIV-EXO vs. CTRL-EXO with molecular functions, biological processes, cellular components, and the KEGG pathway.

REFERENCES

1. Capua I, Marangon S. Control of avian influenza in poultry. *Emerg Infect Dis*. 2006;12(9):1319-1324. PUBMED | CROSSREF
2. Tumpey TM, Belser JA. Resurrected pandemic influenza viruses. *Annu Rev Microbiol*. 2009;63(1):79-98. PUBMED | CROSSREF
3. Khan A, Jahejo AR, Qiao ML, Han XY, Cheng QQ, Mangi RA, et al. NF-κB pathway genes expression in chicken erythrocytes infected with avian influenza virus subtype H9N2. *Br Poult Sci*. 2021;62(5):666-671. PUBMED | CROSSREF
4. Filaire F, Sécula A, Bessière P, Pagès-Homs M, Guérin JL, Violleau F, et al. High and low pathogenicity avian influenza virus discrimination and prediction based on volatile organic compounds signature by SIFT-MS: a proof-of-concept study. *Sci Rep*. 2024;14(1):17051. PUBMED | CROSSREF
5. Charoenviriyakul C, Takahashi Y, Morishita M, Matsumoto A, Nishikawa M, Takakura Y. Cell type-specific and common characteristics of exosomes derived from mouse cell lines: yield, physicochemical properties, and pharmacokinetics. *Eur J Pharm Sci*. 2017;96:316-322. PUBMED | CROSSREF
6. Zhang Y, Liu Y, Liu H, Tang WH. Exosomes: biogenesis, biologic function and clinical potential. *Cell Biosci*. 2019;9(1):19. PUBMED | CROSSREF
7. Bedford JG, Infusini G, Dagley LF, Villalon-Letelier F, Zheng MZM, Bennett-Wood V, et al. Airway exosomes released during influenza virus infection serve as a key component of the antiviral innate immune response. *Front Immunol*. 2020;11:887. PUBMED | CROSSREF
8. Maemura T, Fukuyama S, Sugita Y, Lopes TJS, Nakao T, Noda T, et al. Lung-derived exosomal miR-483-3p regulates the innate immune response to influenza virus infection. *J Infect Dis*. 2018;217(9):1372-1382. PUBMED | CROSSREF
9. Schultz IC, Bertoni APS, Wink MR. Mesenchymal stem cell-derived extracellular vesicles carrying miRNA as a potential multi target therapy to COVID-19: an *in silico* analysis. *Stem Cell Rev Rep*. 2021;17(2):341-356. PUBMED | CROSSREF
10. Liu S, Mok BW, Deng S, Liu H, Wang P, Song W, et al. Mammalian cells use the autophagy process to restrict avian influenza virus replication. *Cell Rep*. 2021;35(10):109213. PUBMED | CROSSREF
11. Yao Z, Qiao Y, Li X, Chen J, Ding J, Bai L, et al. Exosomes exploit the virus entry machinery and pathway to transmit alpha interferon-induced antiviral activity. *J Virol*. 2018;92(24):e01578-18. PUBMED | CROSSREF
12. Vu TH, Heo J, Kang S, Kim C, Lillehoj HS, Hong YH. Chicken miR-26a-5p modulates MDA5 during highly pathogenic avian influenza virus infection. *Dev Comp Immunol*. 2023;149:104921. PUBMED | CROSSREF
13. Umar S, Guerin JL, Ducatez MF. Low pathogenic avian influenza and coinfecting pathogens: a review of experimental infections in avian models. *Avian Dis*. 2017;61(1):3-15. PUBMED | CROSSREF
14. Monne I, Fusaro A, Nelson MI, Bonfanti L, Mulatti P, Hughes J, et al. Emergence of a highly pathogenic avian influenza virus from a low-pathogenic progenitor. *J Virol*. 2014;88(8):4375-4388. PUBMED | CROSSREF
15. Huprikar J, Rabinowitz S. A simplified plaque assay for influenza viruses in Madin-Darby kidney (MDCK) cells. *J Virol Methods*. 1980;1(2):117-120. PUBMED | CROSSREF

16. Hong Y, Lee J, Vu TH, Lee S, Lillehoj HS, Hong YH. Immunomodulatory effects of poly(I:C)-stimulated exosomes derived from chicken macrophages. *Poult Sci*. 2021;100(8):101247. PUBMED | CROSSREF
17. Livak KJ, Schmittgen TD. Analysis of relative gene expression data using real-time quantitative PCR and the $2^{-\Delta\Delta CT}$ method. *Methods*. 2001;25(4):402-408. PUBMED | CROSSREF
18. Hong Y, Truong AD, Vu TH, Lee S, Heo J, Kang S, et al. Profiling and analysis of exosomal miRNAs derived from highly pathogenic avian influenza virus H5N1-infected White Leghorn chickens. *Poult Sci*. 2022;101(11):102123. PUBMED | CROSSREF
19. Wu N, Yang B, Wen B, Wang T, Guo J, Qi X, et al. Interactions among expressed microRNAs and mRNAs in the early stages of fowl adenovirus aerotype 4-infected Leghorn male hepatocellular cells. *Front Microbiol*. 2020;11:831. PUBMED | CROSSREF
20. Wang Y, Brahmakshatriya V, Lupiani B, Reddy SM, Soibam B, Benham AL, et al. Integrated analysis of microRNA expression and mRNA transcriptome in lungs of avian influenza virus infected broilers. *BMC Genomics*. 2012;13(1):278. PUBMED | CROSSREF
21. Yang X, Gao W, Liu H, Li J, Chen D, Yuan F, et al. MicroRNA transcriptome analysis in chicken kidneys in response to differing virulent infectious bronchitis virus infections. *Arch Virol*. 2017;162(11):3397-3405. PUBMED | CROSSREF
22. Hong Y, Truong AD, Lee J, Vu TH, Lee S, Song KD, et al. Exosomal miRNA profiling from H5N1 avian influenza virus-infected chickens. *Vet Res*. 2021;52(1):36. PUBMED | CROSSREF
23. Li H, Shang H, Shu D, Zhang H, Ji J, Sun B, et al. gga-miR-375 plays a key role in tumorigenesis post subgroup J avian leukosis virus infection. *PLoS One*. 2014;9(4):e90878. PUBMED | CROSSREF
24. Zhang W, Liu HT. MAPK signal pathways in the regulation of cell proliferation in mammalian cells. *Cell Res*. 2002;12(1):9-18. PUBMED | CROSSREF
25. Huang G, Shi LZ, Chi H. Regulation of JNK and p38 MAPK in the immune system: signal integration, propagation and termination. *Cytokine*. 2009;48(3):161-169. PUBMED | CROSSREF
26. Krzyzowska M, Swiatek W, Fijalkowska B, Niemialtowski M, Schollenberger A. The role of map kinases in immune response. *Adv Cell Biol*. 2010;2(3):125-138. CROSSREF
27. Cheng Y, Sun F, Wang L, Gao M, Xie Y, Sun Y, et al. Virus-induced p38 MAPK activation facilitates viral infection. *Theranostics*. 2020;10(26):12223-12240. PUBMED | CROSSREF
28. Meineke R, Rimmelzwaan GF, Elbahesh H. Influenza virus infections and cellular kinases. *Viruses*. 2019;11(2):171. PUBMED | CROSSREF
29. Yu J, Sun X, Goie JYG, Zhang Y. Regulation of host immune responses against influenza A virus infection by mitogen-activated protein kinases (MAPKs). *Microorganisms*. 2020;8(7):1067. PUBMED | CROSSREF
30. Briscoe J, Thérond PP. The mechanisms of Hedgehog signalling and its roles in development and disease. *Nat Rev Mol Cell Biol*. 2013;14(7):416-429. PUBMED | CROSSREF
31. Ballester A, Guijarro A, Bravo B, Hernández J, Murillas R, Gallego MI, et al. Hedgehog signalling modulates immune response and protects against experimental autoimmune encephalomyelitis. *Int J Mol Sci*. 2022;23(6):3171. PUBMED | CROSSREF
32. Li Y, Ming M, Li C, Liu S, Zhang D, Song T, et al. The emerging role of the hedgehog signaling pathway in immunity response and autoimmune diseases. *Autoimmunity*. 2023;56(1):2259127. PUBMED | CROSSREF
33. Ding B, Zhang G, Yang X, Zhang S, Chen L, Yan Q, et al. Phosphoprotein of human parainfluenza virus type 3 blocks autophagosome-lysosome fusion to increase virus production. *Cell Host Microbe*. 2014;15(5):564-577. PUBMED | CROSSREF
34. Levine B. Eating oneself and uninvited guests: autophagy-related pathways in cellular defense. *Cell*. 2005;120(2):159-162. PUBMED | CROSSREF